Original Article

MiR-4291 stabilized the vulnerable atherosclerotic plaques by degrading the MAPK1/ERK2 in ApoE$^{-/-}$ mice

Yaqiong Jin^, Jingchao Lu^, Fan Liu^, Xiuchun Yang^, Fei Chen^, Jie Zhang^

Department of Cardiology, The Second Hospital of Hebei Medical University, Shijiazhuang, China

Contributions: (I) Conception and design: Y Jin, J Lu; (II) Administrative support: J Lu; (III) Provision of study materials: F Liu, X Yang; (IV) Collection and assembly of data: Y Jin, J Lu, F Liu; (V) Data analysis and interpretation: X Yang, F Chen, J Zhang; (VI) Manuscript writing: All authors; (VII) Final approval of manuscript: All authors.

Correspondence to: Jingchao Lu. Department of Cardiology, The Second Hospital of Hebei Medical University, Shijiazhuang, China.
Email: lujc66003973@163.com.

Background: This study sought to explore the mechanism of action of the micro ribonucleic acid (miR)-4291 in stabilizing atherosclerotic (AS) plaques.

Methods: An AS model of apolipoprotein E-deficient (ApoE$^{-/-}$) mice fed a high-fat diet (HFD) was established. Oxidized low-density lipoprotein (ox-LDL) was used to induce an inflammatory response of RAW264.7 macrophages. The mice were divided into the normal diet (ND) + miR-4291 negative control (NC) group, the ND + miR-4291 mimic group, the HFD + miR-4291 NC group, and the HFD + miR-4291 mimic group. They were also classified into the miR-4291 NC group, the miR-4291 mimic group, the ox-LDL + miR-4291 NC group, and the ox-LDL + miR-4291 mimic group. The arterial plaque burden of the mice was assessed by hematoxylin-eosin staining and immunohistochemistry, and the expression of phosphorylated-extracellular signal-regulated kinase 2 (p-ERK2) and related proteins in the arterial plaques and RAW264.7 macrophages of the mice were detected by Western blotting.

Results: Obvious plaques with massive macrophage infiltration were found in the aortic roots of the mice fed a HFD, and smooth muscle cells were found at the margin of the plaques. In the HFD + miR-4291 mimic group, the number of plaques and macrophages was significantly declined, but there were no significant changes in the smooth muscle cells compared to those in the HFD + miR-4291 NC group. The Western blot results showed that miR-4291 reduced the protein expression of p-ERK1-2, t-ERK1-2, TNF-α, MCP-1, MMP-1, MMP-3, and MMP-9 in the AS plaques and the ox-LDL-induced RAW264.7 macrophages of the mice fed a HFD.

Conclusions: MiR-4291 reduced the expression of MMP-2/9 by inhibiting the activity of ERK2, which in turn increased the fibrous cap thickness and stabilized the vulnerable plaques in AS.

Keywords: miR-4291; p-ERK1-2; fibrous cap thickness; vulnerable plaques

Submitted Sep 21, 2022. Accepted for publication Nov 17, 2022.
doi: 10.21037/atm-22-5241
View this article at: https://dx.doi.org/10.21037/atm-22-5241

^ ORCID: Yaqiong Jin, 0000-0001-8440-0236; Jingchao Lu, 0000-0002-8398-4943; Fan Liu, 0000-0002-6424-4157; Xiuchun Yang, 0000-0002-1096-7237; Fei Chen, 0000-0002-9544-213X; Jie Zhang, 0000-0002-4057-109X.

Introduction

Atherosclerosis (AS), which is the major pathological cause of cardiovascular diseases in adults, may lead to myocardial infarction or stroke, resulting in death (1). Thrombosis after AS plaque erosion and rupture is one of the major pathogeneses of clinical cardiovascular events (2). AS plaques that are primarily composed of surface fibrous caps and lipid cores inside are characterized by smooth muscle cell (SMC) proliferation and inflammatory cell infiltration (3). Plaque stability is determined by the composition of the plaque, and unstable plaques have a higher risk of rupture. The fibrous cap thickness of AS plaques is one of the main determinants of plaque vulnerability. The formation of plaque fibrous caps, the maintenance of their integrity, and their resistance to rupture are heavily dependent on the extracellular matrix (ECM) (4).

Matrix metalloproteinases (MMPs) are the most important known ECM-degrading enzymes (5). MMPs can promote the migration of macrophages and vascular SMCs in the intima by degrading the basement membrane of endothelial cells. Macrophages invade tissues by multiple pathways and can cause damage to AS plaques (6). Oxidized low-density lipoprotein (ox-LDL) can induce inflammation in macrophages, and the expression of pro-inflammatory factors, such as tumor necrosis factor-α (TNF-α), is high in the macrophages and SMCs (7). MMPs can also promote the release of cytokines, such as monocyte chemoattractant protein-1 (MCP-1) and TNF-α, by macrophages and these cytokines in turn enhance the activity of MMPs, such that positive feedback regulation results, which further worsens the inflammation around the plaque, and accelerates plaque rupture (8).

MMPs best reflect the pathophysiology of vulnerable plaques, and can even serve as surrogate endpoints for predicting plaque vulnerability (9). Thus, the level and expression intensity of MMPs (MMP-1/2/9) provides an indication of the deterioration degree of vulnerable plaques. Extracellular signal-regulated kinase (ERK) can transmit extracellular information to the nucleus through phosphorylation, facilitating the transcriptional activation of cell proliferation- and differentiation-related proteins (10). The excessive activation of ERK2 and the high expression of MMP-2/3/9 are also associated with AS (9,11,12).

On the other hand, plaque formation and inflammatory activate endothelial repair mechanism and angiogenesis process. The unproperly repairing of endothelial cells causes destructive inflammation, aging of arterial wall, and abnormal remodeling of vascular wall (13); the dysfunctional repair mechanism accompanied by abnormal even damaged pathological neovascularization increase the plaque vulnerability, aggravate the formation of plague, thus accelerate the progression of AS (14-16). Moreover, the microenvironment of vulnerable plaques also plays important roles in AS (17), and the systemic treatment for AS has been exploring to reduce unfavorite clinical outcome (17,18).

Micro RNAs (miRNAs) induce the degradation or translation inhibition of messenger RNAs (mRNAs) by binding to the 3 prime untranslated regions of the target mRNAs, which leads to the post-transcriptional regulation of proteins (19,20). In recent years, the important regulatory role of miRNAs in a variety of physiological and pathological processes, including the AS process, has been confirmed in a number of studies (21,22). Research have indicated the miR-214 family members play important roles in AS (23,24). The microarray hybridization analysis indicated that the highly homologous mRNA or microRNA family could combine with the same target to affect its effect (25). The length of mature miR-4291 is 16 bp and is considered as one member of miR-214 family (25). A recent report (26) showed it was obvious differentially expressed in abdominal aortic aneurysms, compared with normal tissue. This inspired us to explore the role of miR-4291, which is rarely reported, in AS. In the present study, we established an AS model of apolipoprotein E-deficient ($ApoE^{-/-}$) mice fed a high-fat diet (HFD) to explore the mechanisms of the microRNA (miR)-4291 in stabilizing AS plaques, and in the ox-LDL-induced inflammatory response in

Highlight box

Key findings

- Decreased miR-4291 in atherosclerosis reduced the expression of MMP-2/9 and inhibits the activity of ERK2, which in turn increased the fibrous cap thickness and stabilized the vulnerable plaques in atherosclerosis. Upregulation of miR-4291 declines the number of plaques and macrophages *in vitro* and *in vivo*.

What is known and what is new?

- Thrombosis after atherosclerosis plaque erosion and rupture is a major pathogenesis of clinical cardiovascular events.
- Compelling studies indicated that microRNAs are involved in regulating the atherosclerosis process, which affects the function of vascular wall cells.

What is the implication, and what should change now?

- This study provides a basis for the application of microRNAs in the development and treatment of atherosclerosis in the future.

RAW264.7 macrophages cultured *in vitro*. We present the following article in accordance with the ARRIVE reporting checklist (available at https://atm.amegroups.com/article/view/10.21037/atm-22-5241/rc).

Methods

Data and bioinformatics analysis methods

Bioinformatics analysis

The Gene Expression Omnibus (GEO) database (https://www.ncbi.nlm.nih.gov/gds/) was searched for AS-related data sets, and the AS-related mRNA gene expression GSE9874 data set was found and downloaded. The miRNA sequencing GSE59421 data set for AS patients was also downloaded. The study was conducted in accordance with the Declaration of Helsinki (as revised in 2013). The quantile RNA-sequencing data was standardized using R language limma package, and a |log fold change [FC]| <1 and a P value <0.05 indicated a statistically significant difference in the gene analysis. The Ggplot2 software package in R software was used to construct a volcano map in which the differentially expressed genes (DEGs) in the GSE9874 data set were grouped, and pheATMap software package was used to draw the cluster analysis heatmap of the DEGs. Similarly, volcanic maps and cluster analysis heat maps were used to group the DEGs for the GSE59421 data set.

Functional enrichment analyses

Gene Ontology (GO) and Kyoto Encyclopedia of Genes and Genomes (KEGG) enrichment analyses were conducted for the DEGs in the GSE9874 data set. Using the online database tool DAVID (https://david.ncifcrf.gov), the 3 levels for the DEGs (i.e., the cellular composition, molecular function and biological process) were analyzed by integrating the GO terms, network, and the DEGs of a biological process. The GOplot and GGplot2 packages were used to map the GO pathway and enrichment analysis diagram of the KEGG pathways of the DEGs in the R linguistic environment.

Gene Set Enrichment Analysis (GSEA)

The GSEA tool (http://www.gsea-msigdb.org/) was used to conduct a GSEA of all the genes, and the GSEA enrichment analysis pathways was mapped.

miRNA target gene prediction

The miRNA candidate target genes were predicted by miRDB, the online tool targetScan, and a venn diagram was drawn using the VennDiagram package together with the GSE59421 DEGs. The binding sites of the mRNAs and miRNAs were mapped according to the gene prediction results.

In vivo experimental design

Animal feeding and modeling

The ApoE$^{-/-}$ mice with a C57BL/6 background purchased from skbex biotechnology, were randomly divided into the following 4 groups (n=7 per group): (I) the chow diet (CD) + miR-4291 negative control (NC) group; (II) the CD + miR-4291 mic group; (III) the HFD + miR-4291 NC group; and 4) the HFD + miR-4291 mic group. The mice were fed a HFD and CD and kept on 12-h light/dark cycle. The AS mouse model was established by feeding the mice a HFD containing 15% cocoa butter + 0.25% cholesterol for 12 weeks. The expression of miR-4291 in the mice was disturbed by a tail vein injection of miR-4291 mimic, and a tail vein injection of miR-4291 NC was used as the negative control.

At the end of the experiment, all the mice were anesthetized by an intraperitoneal injection of sodium pentobarbital, and the mice were killed by taking blood from the cardiac apex. After perfusion with normal saline, the aorta and heart were completely stripped. The aortic roots of 3 mice in each group were randomly selected and fixed in 4% paraformaldehyde for 12 h. The aortic roots were embedded with optimal cutting temperature (OCT) and made into frozen sections for pathomorphological examination. The aortas of the other mice were directly put into liquid nitrogen and then transferred to –80℃ for the molecular biological analysis.

All protocols were prepared without registration before the study and reviewed by the member of the Ethics Committee. All the animal procedures were performed following the National Institutes of Health (NIH) Guide for the Care and Use of Laboratory Animals and were approved by the Ethics Review Committee of Hebei Medical University (approval No. 2022-AE115).

Oil red O staining

The whole length of each aorta was observed under a gross microscope. The adventitia was stripped, and the blood vessels were cut longitudinally. An oil red O working solution was prepared, and the blood vessels were soaked at room temperature for 2 h. The blood vessels were then

transferred to warm water and observed in real time under a microscope until the plaque was red and the normal tube wall was white. The floating color on the blood vessel surface was washed with distilled water, the blood vessel was flattened by pressing the cover glass and photographs were taken, and blood vessel microscopic figures. were measured with Image Pro Plus 5.0 software image analysis software.

H&E staining of the aortic roots

The paraffin slides were stained with hematoxylin blue and differentiated with 1% hydrochloric-acid alcohol for 5 seconds. The staining was observed under the microscope. After washing with tap water, the nuclei were dark blue, and the cytoplasm was not stained under the microscope. Next, eosin staining was used, gradient-concentration alcohol and xylene were used to dehydrate and finally, the neutral gum was sealed. Nuclear blue was visible under the microscope. After the film was dried, it was photographed and measured by Image Pro Plus 5.0 software.

Immunohistochemistry

Paraffin sections were dehydrated using graded ethanol. After hydration, the tissue was marked with an immunohistochemical pen, the slide was placed in a wet box, 3% Hydrogen peroxide (H_2O_2) was dripped to cover the tissue, and the tissue was incubated at room temperature for 10 min. After cleaning with phosphate buffered solution (PBS), 5% bovine serum albumin (BSA) solution was added dropwise to the tissue surface and tissue sections were sealed at room temperature for 30 min. The tissue surface blocking solution was discarded, and the diluted primary antibody [cluster of differentiation 68 $(CD68)^+$ and Alpha-smooth muscle actin (α-SMA) was then added and incubated overnight at 4 ℃. The next day, the secondary antibody was incubated according to the relevant steps of the corresponding immunohistochemical detection kit. After PBS cleaning, the DAB was stained and dark yellow granules could be observed in the tissue under the microscope. The slide was immersed in tap water to terminate the staining. Next, hematoxylin was stained, sections were washed with tap water to remove the floating color, 1% hydrochloric-acid alcohol was differentiated for 5S, and then sections washed with running water to return to blue. Gradient alcohol and xylene were used to achieve dehydration and transparency. Finally, the neutral gum was sealed, dried overnight, observed, and photographed under the microscope, and measured with Image Pro Plus 5.0 software.

In vitro experimental design

Cell culture and transfection

RAW264.7, the mouse macrophage cell line, was placed in Dulbecco's Modified Eagle Medium (DMEM) medium containing 10% fetal bovine serum, 100 mmol/L of penicillin, and 100 mmol/L of streptomycin, and cultured in a 5% carbon dioxide incubator at 37 ℃, and sub-cultured once every 1–2 days. The cells in the logarithmic growth period were used for the experiment. Mir-4291 mimic and miR-4291 NC were transfected into the RAW264.7 cells, respectively, using Lipo2000. The cells in the logarithmic growth stage were digested and counted, and the suspension concentration was adjusted to 5×10^5 cells/mL. The cells were then inoculated into 6-well plates, and 2 mL of DMEM complete medium was added to each well. When the cells covered about 70% of the bottom area of the plate they were divided into the miR-4291 NC group, miR-4291 mimic group, ox-LDL + miR-4291 NC group and ox-LDL + miR-4291 mimic group. In the ox-LDL group, 50 mg/L of ox LDL was added to induce the inflammation of the RAW264.7 macrophages.

Western blot

The RAW264.7 cells and descending aortic tissue/proteins from the $ApoE^{-/-}$ mice were collected. The plaque tissue was separated with a sterilized glass needle. After homogenization, the supernatant was extracted. The total protein concentration of the cells and tissues was measured using the BCA method. After loading samples sodium dodecyl sulfate–polyacrylamide gel electrophoresis and membrane transfer were carried out. The transferred membranes were then blocked with 5% skimmed milk powder for 2 h. The cells were incubated with the primary antibodies (p-ERK1-2, t-ERK1-2, MCP-1, MMP-1, TNF-α, MMP-3, MMP-9, and β-actin) overnight at a constant temperature level of 4℃. After washing the membranes, the transferred membranes were incubated at room temperature for 2 hours (1:5,000). The gel imaging system Enhanced Chemiluminescence (ECL) was used to get pictures, and the experiment was repeated 3 times. The relative expression of protein was compared to the corresponding internal parameters by ImageJ software.

Statistical analysis

SPSS 23.0 software was used for the statistical analysis. The measurement data of the animal experiments and *in vitro*

experiments are expressed as the mean ± standard deviation (SD), or the mean ± mean of standard error (SEM). A 1-way analysis of variance was used for each group, and the least significant difference (LSD) test was used for the pairwise comparisons. P values <0.05 and <0.01 were considered statistically significant.

Results

Screening of the DEGs

The GSE9874 data set related to AS was downloaded from the GEO database, and the data were subjected to quantile normalization (*Figure 1A*,*1B*), after which the GSE9874 data set was screened. A P value <0.05 and a |log FC| <1 were considered statistically significant. The results showed that there were 135 DEGs in the mRNAs of AS, of which 71 were upregulated and 64 were downregulated. The volcano plot grouping of the DEGs in the GSE9874 data set was constructed using the ggplot2 package of R software (*Figure 1C*), and the cluster analysis heat map of the DEGs was plotted using the pheatmap package of R software (*Figure 1D*). Additionally, the miRNAs in the GSE59421 data set were subjected to quantile normalization (*Figure 1E,1F*), the DEGs were screened, and the volcano plot (*Figure 1G*) and cluster analysis heat map of the DEGs (*Figure 1H*) were constructed in the same methods as GSE9874.

Bioinformatics analysis

The DEGs obtained from the GSE9874 data set were subjected to GO and KEGG enrichment analyses. The DEGs at the biological process level were analyzed using the online database tool DAVID (https://david.ncifcrf.gov/) to integrate the GO terms, and the biological process network of the DEGs was created. Diagrams of the upregulated GO pathways (*Figure 1I*,*1J*) and the downregulated pathways (*Figure 1K*,*1L*) of the DEGs were plotted using R language. The related upregulated and downregulated pathways were the enriched pathways of AS. A KEGG pathway analysis of the DEGs was conducted, and the KEGG pathway diagram was plotted (*Figure 1M*).

Prediction of miRNA target genes

The candidate miRNA target genes were predicted using the online tools miRDB and TargetScan. The miRNA target genes were plotted in a Venn diagram with the DEGs from the GSE59421 data set using the Venn Diagram package, and the possible intersection targets were analyzed. Then miR-4291 was found to possible bind to all DEGs (*Figure 1N*). The binding sites between the mRNAs and miRNAs were also plotted based on the prediction results (*Figure 1O*).

GSEA

The GSEA showed that the ERK signaling pathway was enriched (*Figure 1P*,*1Q*).

Histomorphological observations of the mouse aortas

The intravascular plaque burden was displayed by oil Red O staining (*Figure 2*) and hematoxylin and eosin (H&E) staining of the aortic roots (*Figure 3A*). Obvious plaques were observed in the aortic roots of the mice fed the HFD compared to those fed a normal diet (ND). The plaques were significantly more reduced in the HFD + miR-4291 mimic group than the HFD + miR-4291 NC group.

MiR-4291 reduced the content of CD68 in the macrophages in the AS plaques

Immunohistochemical staining was performed on the CD68 in the macrophages in the AS plaques using frozen sections of the aortic roots (*Figure 3B*). The results revealed that there was massive macrophage infiltration in the plaques of the mice fed HFD. The number of macrophages in the AS plaques was significantly decreased in the HFD + miR-4291 mimic group compared to that in the HFD + miR-4291 NC group.

Number of SMCs in the AS plaques

As shown in *Figure 3C*, the α-SMA-specific immunohistochemical staining showed SMCs in the plaques of the mice fed a HFD, which were mainly distributed in the margin of the plaques. However, there was no obvious change in the number of SMCs in the AS plaques between the HFD + miR-4291 NC group and the HFD + miR-4291 mimic group.

MiR-4291 lowered the protein expression of p-ERK1-2, t-ERK1-2, MCP-1, MMP-1, TNF-α, MMP-3, and MMP-9 in the AS plaques and RAW264.7 cells

As shown in *Figure 4*, the protein expression of p-ERK1-2, MCP-1, MMP-1, TNF-α, MMP-3, and MMP-9 in the

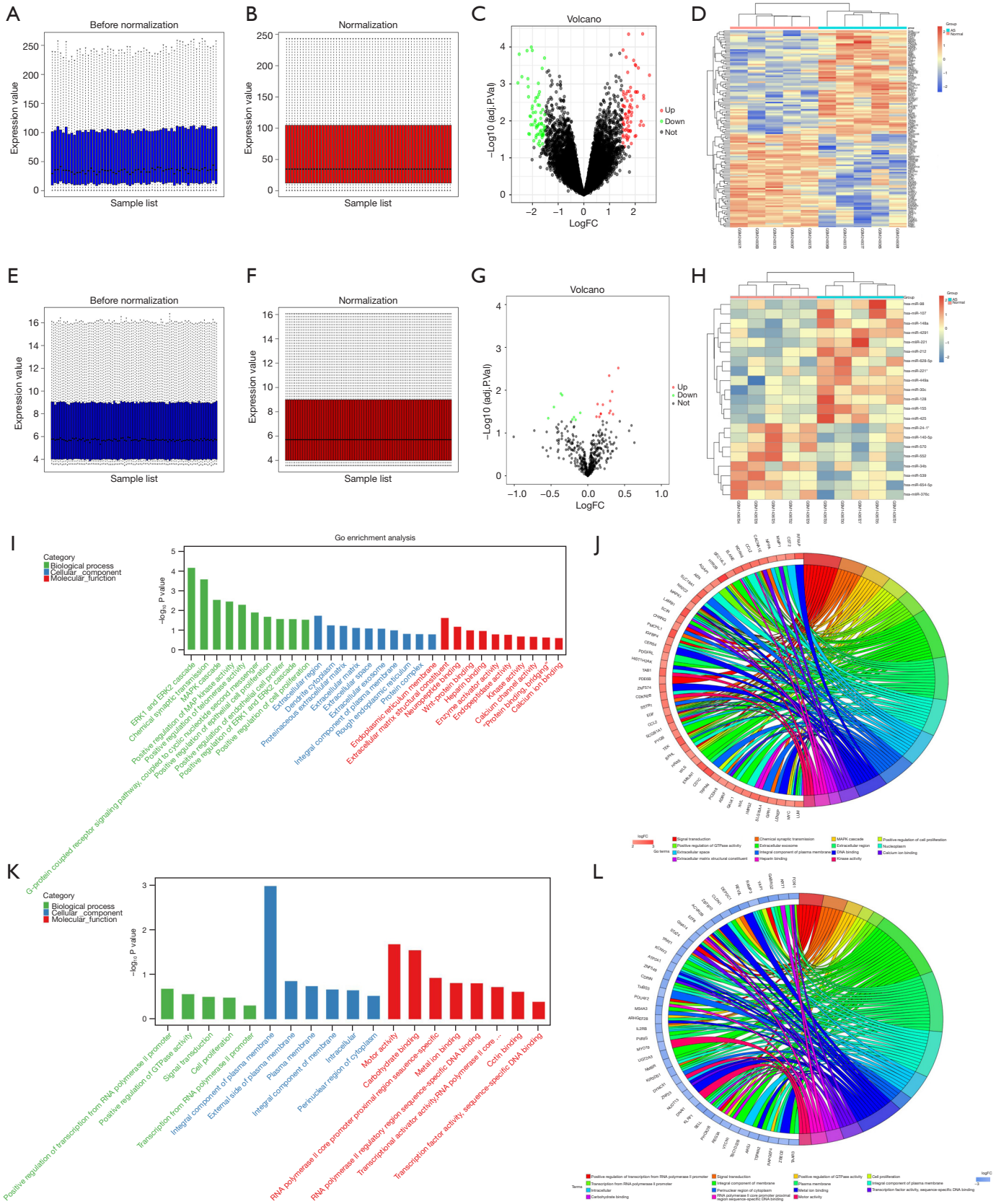

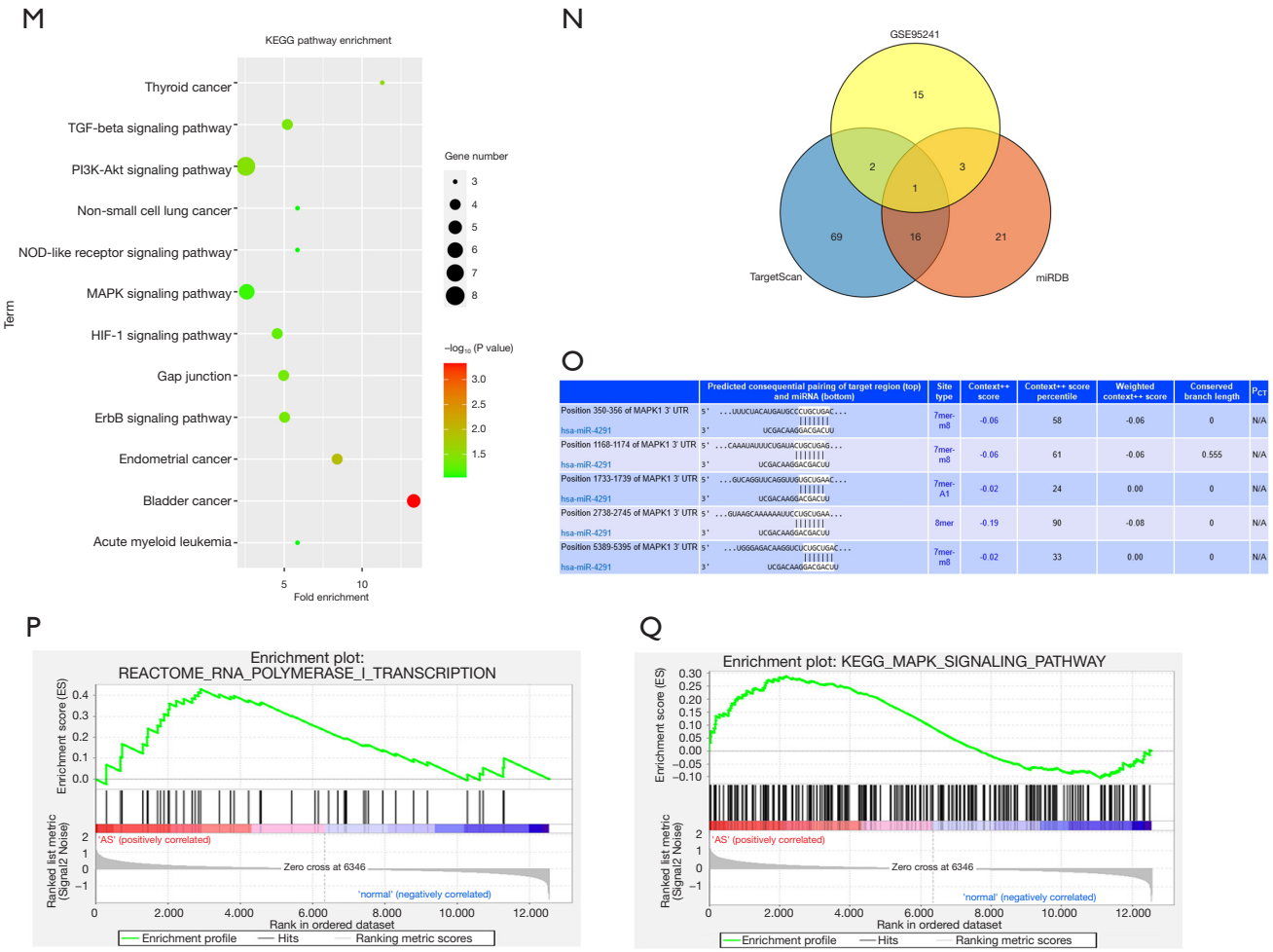

Figure 1 Bioinformatics analysis. (A,B) Quantile normalization of data set GSE9874. (C,D) Volcano plot and cluster analysis heat map of the DEGs in GSE9874. (E,F) Quantile normalization of GSE59421 data set of the miRNAs. (G,H) Volcano plot and cluster analysis heat map of the DEGs in GSE59421. (I,J) Upregulated GO pathways. (K,L) Downregulated GO pathways. (M) KEGG pathways. (N) Venn diagram. (O) Binding sites between mRNAs and miRNAs. (P,Q) GSEA. *, P<0.05. DEGs, differentially expressed genes; GO, gene ontology; miRNA, micro RNA; mRNA, messenger RNA; KEGG, Kyoto encyclopedia of genes and genomes; GSEA, gene set enrichment analysis.

AS plaques were significantly increased in the mice fed a HFD compared to those fed a ND. The expression of t-ERK1-2 significantly declined, while the expression of other proteins showed no obvious changes in the ND + miR-4291 mimic group compared to the ND + miR-4291 NC group. MiR-4291 reduced the protein expression of p-ERK1-2, t-ERK1-2, MCP-1, MMP-1, TNF-α, MMP-3, and MMP-9 in the AS plaques of the mice fed a HFD. Consistent with the *in vivo* experiment results, as shown in *Figure 5*, The expression of t-ERK1-2 declined significantly, while the expression of other proteins showed no obvious changes in the miR-4291 mimic group compared to the miR-4291 NC group. Additionally, the ox-LDL + miR-4291 mimic group had significantly lower protein expression of p-ERK1-2, t-ERK1-2, MCP-1, MMP-1, TNF-α, MMP-3, and MMP-9 in the ox-LDL-induced RAW264.7 macrophages than the ox-LDL + miR-4291 NC group.

Discussion

AS is a chronic progressive inflammatory disease (27,28), and AS-induced clinical events, such as myocardial infarction are stroke, are primarily triggered by thrombosis

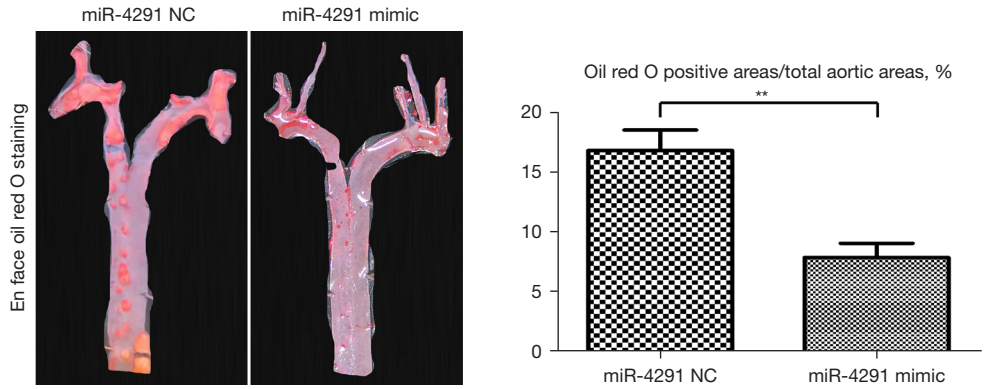

Figure 2 Oil Red O staining (×10) for the miR-4291 NC and mimic group, the ratio of oil red O positive areas to total aortic areas. **, P<0.01 was considered statistically significant. The data are expressed as the mean ± SD of 7 separate experiments. NC, negative control; SD, standard deviation.

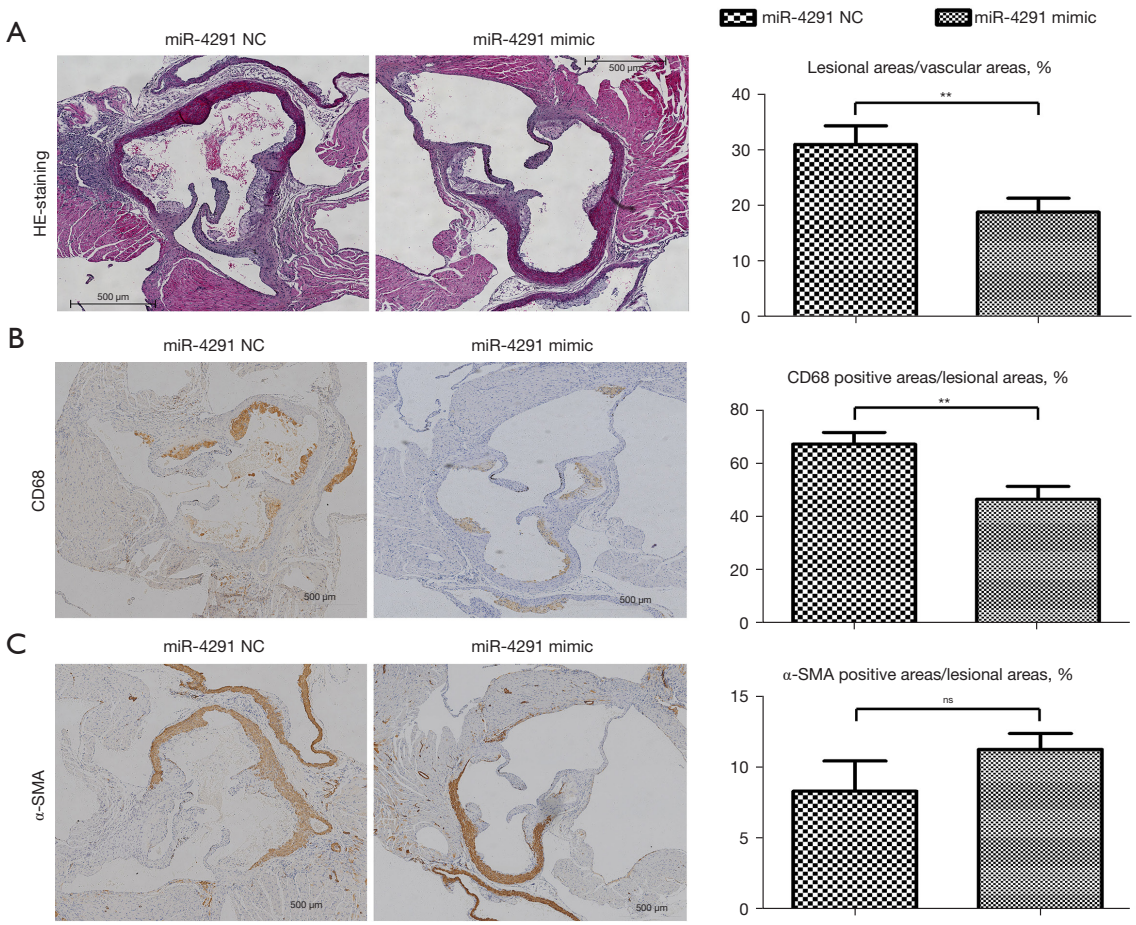

Figure 3 H&E staining of mouse aortic roots and specific immunohistochemical staining. (A) Histomorphological observation of mouse aortic roots. (B) Content of CD68 in macrophages in AS plaques. Yellow staining indicates positive results. (C) Number of SMCs in the AS plaques detected by α-SMA-specific immunohistochemical staining. Yellow staining indicates positive results. The data are expressed as the mean ± SD for the 7 separate experiments. **, P<0.01 was considered statistically significant. NC, negative control; ns, not significant; AS, atherosclerosis.

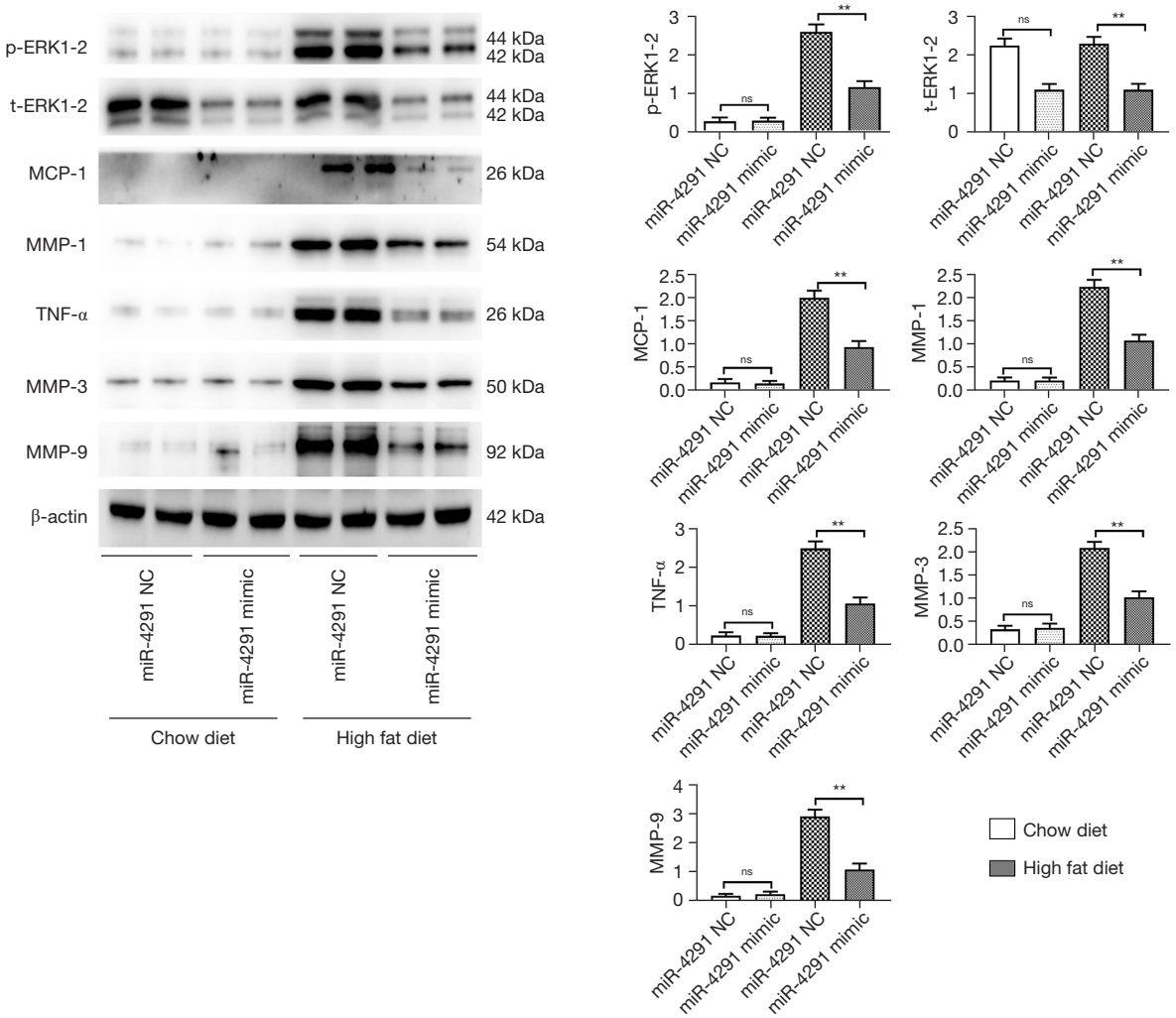

Figure 4 Protein expression of p-ERK1-2, t-ERK1-2, MCP-1, MMP-1, TNF-α, MMP-3, and MMP-9 in the mouse AS plaques. **, P<0.01 was considered statistically significant. The data are expressed as the mean ± SD for the 7 separate experiments. NC, negative control; ns, not significant; AS, atherosclerosis; SD, standard deviation.

resulting from acute plaque rupture or the erosion of unstable plaques. Thus, there is a close association between AS plaque stability and clinical cardiovascular (CV) events (2). To reduce the occurrence of CV event, imaging detecting arterial plaque and necessary drug therapy including antiplatelet and statin drugs are important methods to prevent and treat AS plaque. However, the "residual risk" of AS remains high (18,29-31) make it necessary to further consolidate the current prevention and control strategy by other means. At present, the classification of vulnerable plaque needs to be further subdivided (18). The systemic treatment including anti-inflammatory or low-density lipoprotein–lowering are explored to reduced unfavorite clinical outcome in future (18,32). MiRNAs are important regulators of a variety of physiological and pathological processes, and are also involved in regulating the AS process, which affects the function of vascular wall cells (17,33-35). These studies also provide a basis for the application of microRNAs in the development and treatment of AS in the future.

In the present study, DEGs were identified from the GEO database, the candidate miRNA target genes were predicted using TargetScan and mirDIP, and together with DEGs in GSE59421, they were plotted in a Venn diagram using the VennDiagram package. The possible target intersection was analyzed and miR-4291 was found to bind to all the DEGs.

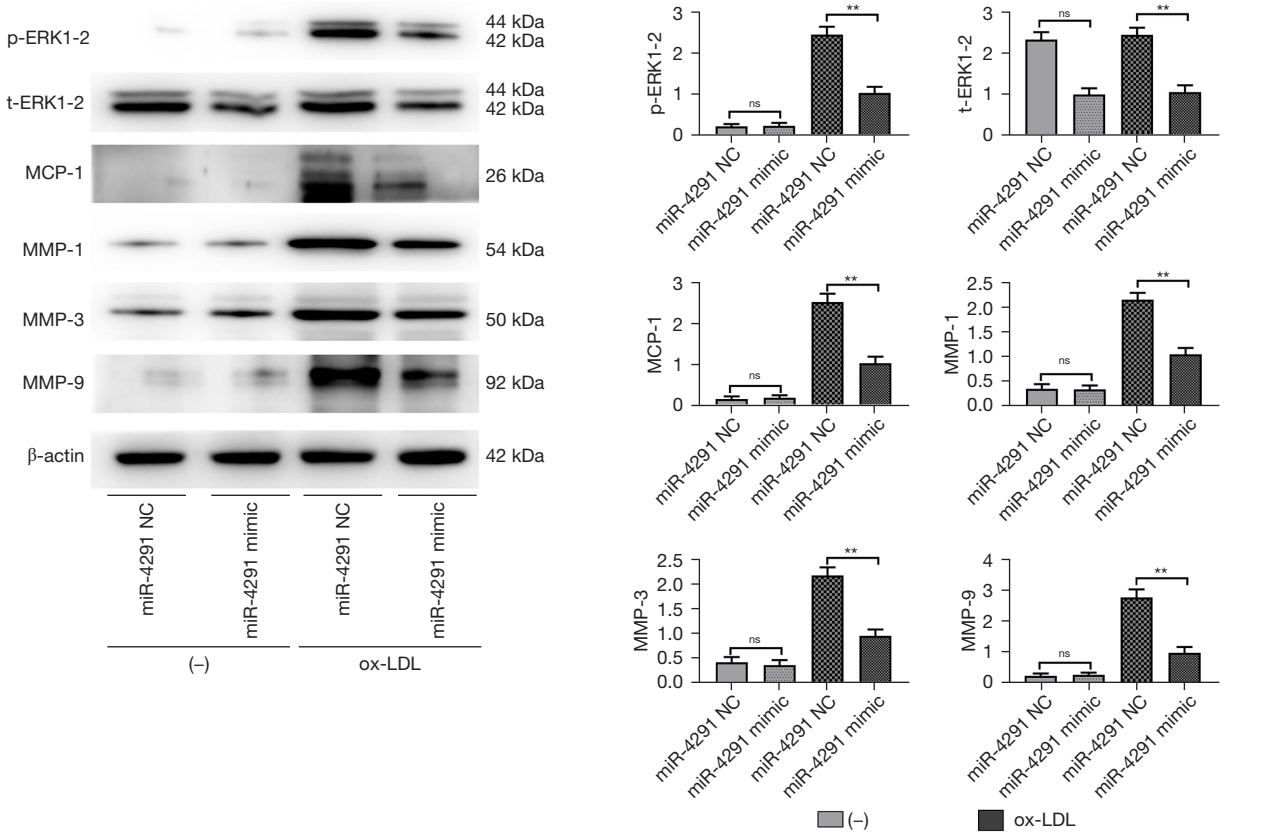

Figure 5 Protein expression of p-ERK1-2, t-ERK1-2, MCP-1, MMP-1, MMP-3, and MMP-9 in the RAW264.7 cells. **, P<0.01 was considered statistically significant. The data are expressed as the mean ±SEM for the 3 separate experiments. NC, negative control; ns, not significant; ox-LDL, oxidized low-density lipoprotein; SEM, standard error of the mean.

The binding sites between the mRNAs and miRNAs were also plotted based on the prediction results. An AS model of ApoE$^{-/-}$ mice was established to explore the effect of miR-4291 overexpression on plaque stability and its mechanism of action.

Plaque stability is primarily determined by the size of the lipid core in the plaque, the degree of inflammatory response, the fibrous cap thickness, and the content of SMCs and macrophages. Endothelial cells, macrophages, and SMCs are implicated in the formation and development of AS plaques, and their functions are closely related to the determinants of plaque stability. The inflammatory response theory is an important theory about the pathogenesis of AS.

Macrophages, the main inflammatory cells, are involved in the formation and development of AS, and play an important role in different stages of AS (36). Fibrous cap thickness is mainly determined by the content of the ECMs and the number of SMCs and macrophages in the plaques. There are often less ECMs and SMCs with macrophage infiltration in vulnerable plaques with thin fibrous caps. In this study, the intravascular plaque burden was assessed by H&E staining of the aortic root and specific immunohistochemistry. The H&E staining results showed that there were obvious plaques in the aortic roots of the mice fed a HFD compared to those fed a ND. The plaques were significantly more reduced in the HFD + miR-4291 mimic group than the HFD + miR-4291 NC group.

The CD68 and α-SMA-specific immunohistochemical staining revealed massive macrophage infiltration, and that the SMCs were mainly distributed at the margin of the plaques in mice fed a HFD. MiR-4291 reduced the number of macrophages in the AS plaques of the mice fed a HFD but had no significant effect on the SMCs. The above findings suggest that miR-4291 stabilizes vulnerable plaques by reducing macrophage infiltration (*Figure 6*).

The protein expression of p-ERK1-2, t-ERK1-2, MCP-1,

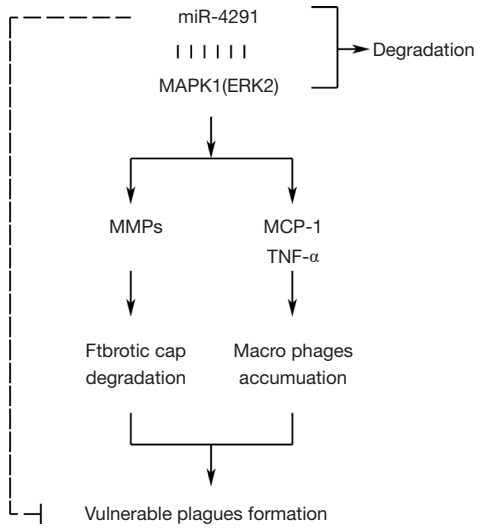

Figure 6 MiR-4291 reduces inflammatory factors by combining and degrading MAPK1 (ERK2), resulting in the decreased secretion of MCP-1, TNF-α, etc. miR-4291 also alleviates the inflammatory response induced by the massive aggregation of macrophages. miR-4291 can also reduce the expression of MMPs and degrade the fibrous cap, resulting in the stabilization of vulnerable plaque. MMP, matrix metalloproteinase.

MMP-1, TNF-α, MMP-3, and MMP-9 in the AS plaques and RAW264.7 macrophages were further detected and combined with the GSEA results. MMPs can promote the migration of macrophages and vascular SMCs in the intima by degrading the basement membranes of endothelial cells. Macrophages that invade tissues by multiple pathways can cause damage to AS plaques (37). In this study, miR-4291 reduced the protein expression of p-ERK1-2, t-ERK1-2, MMP-1, MMP-3, and MMP-9 in the AS plaques and the ox-LDL-induced RAW264.7 macrophages of the mice fed a HFD, indicating that miR-4291 inhibits the activity of ERK2 and reduces the worsening of vulnerable plaques.

MMPs can also promote the release of cytokines, such as MCP-1 and TNF-α, by macrophages and these cytokines in turn enhance the activity of MMPs, such that positive feedback regulation results, which further worsens the inflammation around the plaque, and accelerates plaque rupture (8). We found that miR-4291 inhibited the activity of ERK2, and the secretion of its downstream inflammatory factors TNF-α and MCP-1 was decreased, indicating that miR-4291 reduced the secretion of inflammatory factors (e.g., TNF-α and MCP-1) by macrophages by inhibiting the activity of ERK2, which in turn relieved the inflammatory response induced by massive monocyte aggregation, and enhanced plaque stability (38). However, these findings were based on animal models, and thus may not apply to the complex humans framework. Our study has limitations, in how much degree can miR-4291 inhibit the ERK/MAPK signal pathway, and how about the inhibition effect of miR-4291 compared with the ERK/MAPK pathway inhibitors still need to be further investigated.

Conclusions

In conclusion, miR-4291 reduced macrophage infiltration and inhibited the activity of ERK2, thereby increasing the fibrous cap thickness and stabilizing vulnerable plaques in AS.

Acknowledgments

Funding: The study was supported by the Youth Science and Technology Project of Hebei Health Commission (No. 20190568).

Footnote

Reporting Checklist: The authors have completed the ARRIVE reporting checklist. Available at https://atm.amegroups.com/article/view/10.21037/atm-22-5241/rc

Data Sharing Statement: Available at https://atm.amegroups.com/article/view/10.21037/atm-22-5241/dss

Conflicts of Interest: All authors have completed the ICMJE uniform disclosure form (available at https://atm.amegroups.com/article/view/10.21037/atm-22-5241/coif). The authors have no conflicts of interest to declare.

Ethical Statement: The authors are accountable for all aspects of the work in ensuring that questions related to the accuracy or integrity of any part of the work are appropriately investigated and resolved. All the animal procedures were performed following the NIH Guide for the Care and Use of Laboratory Animals and were approved by the Ethics Review Committee of Hebei Medical University (approval No. 2022-AE115). The study was conducted in accordance with the Declaration of Helsinki (as revised in 2013).

Open Access Statement: This is an Open Access article

References

1. Li J, Ding F, Qian X, et al. Anti-inflammatory cytokine IL10 loaded cRGD liposomes for the targeted treatment of atherosclerosis. J Microencapsul 2021;38:357-64.
2. Shabani M, Bakhshi H, Ostovaneh MR, et al. Temporal change in inflammatory biomarkers and risk of cardiovascular events: the Multi-ethnic Study of Atherosclerosis. ESC Heart Fail 2021;8:3769-82.
3. Pang J, Cheng WL, Peng J, et al. Efficacy of Qingre Huayu Fang on atherosclerotic vulnerable plaque in apolipoprotein E knockout mice: proteasome pathway involvement. J Tradit Chin Med 2021;41:432-7.
4. Lusis AJ. Atherosclerosis. Nature 2000;407:233-41.
5. Nosrati R, Kheirouri S, Ghodsi R, et al. The effects of zinc treatment on matrix metalloproteinases: A systematic review. J Trace Elem Med Biol 2019;56:107-15.
6. Ruddy JM, Ikonomidis JS, Jones JA. Multidimensional Contribution of Matrix Metalloproteinases to Atherosclerotic Plaque Vulnerability: Multiple Mechanisms of Inhibition to Promote Stability. J Vasc Res 2016;53:1-16.
7. Li J, Meng Q, Fu Y, et al. Novel insights: Dynamic foam cells derived from the macrophage in atherosclerosis. J Cell Physiol 2021;236:6154-67.
8. Shalhoub J, Viiri LE, Cross AJ, et al. Multi-analyte profiling in human carotid atherosclerosis uncovers pro-inflammatory macrophage programming in plaques. Thromb Haemost 2016;115:1064-72.
9. Loftus IM, Naylor AR, Bell PR, et al. Matrix metalloproteinases and atherosclerotic plaque instability. Br J Surg 2002;89:680-94.
10. Zou J, Lei T, Guo P, et al. Mechanisms shaping the role of ERK1/2 in cellular senescence (Review). Mol Med Rep 2019;19:759-70.
11. Pott GB, Tsurudome M, Bamfo N, et al. ERK2 and Akt are negative regulators of insulin and Tumor Necrosis Factor-α stimulated VCAM-1 expression in rat aorta endothelial cells. J Inflamm (Lond) 2016;13:6.
12. Zhang S, Xin H, Li Y, et al. Skimmin, a Coumarin from Hydrangea paniculata, Slows down the Progression of Membranous Glomerulonephritis by Anti-Inflammatory Effects and Inhibiting Immune Complex Deposition. Evid Based Complement Alternat Med 2013;2013:819296.
13. Wang D, Li LK, Dai T, et al. Adult Stem Cells in Vascular Remodeling. Theranostics 2018;8:815-29.
14. Jaipersad AS, Lip GY, Silverman S, et al. The role of monocytes in angiogenesis and atherosclerosis. J Am Coll Cardiol 2014;63:1-11.
15. Liu Y, Yu X, Zhang W, et al. Mechanistic insight into premature atherosclerosis and cardiovascular complications in systemic lupus erythematosus. J Autoimmun 2022;132:102863.
16. Nguyen TK, Paone S, Chan E, et al. Heparanase: A Novel Therapeutic Target for the Treatment of Atherosclerosis. Cells 2022;11:3198.
17. Zhang S, Liu Y, Cao Y, et al. Targeting the Microenvironment of Vulnerable Atherosclerotic Plaques: An Emerging Diagnosis and Therapy Strategy for Atherosclerosis. Adv Mater 2022;34:e2110660.
18. Bom MJ, van der Heijden DJ, Kedhi E, et al. Early Detection and Treatment of the Vulnerable Coronary Plaque: Can We Prevent Acute Coronary Syndromes? Circ Cardiovasc Imaging 2017;10:e005973.
19. Gong D, Zhang Q, Chen LY, et al. Coiled-coil domain-containing 80 accelerates atherosclerosis development through decreasing lipoprotein lipase expression via ERK1/2 phosphorylation and TET2 expression. Eur J Pharmacol 2019;843:177-89.
20. Bartel DP. MicroRNAs: target recognition and regulatory functions. Cell 2009;136:215-33.
21. Pu M, Chen J, Tao Z, et al. Regulatory network of miRNA on its target: coordination between transcriptional and post-transcriptional regulation of gene expression. Cell Mol Life Sci 2019;76:441-51.
22. Eken SM, Jin H, Chernogubova E, et al. MicroRNA-210 Enhances Fibrous Cap Stability in Advanced Atherosclerotic Lesions. Circ Res 2017;120:633-44.
23. Lu HQ, Liang C, He ZQ, et al. Circulating miR-214 is associated with the severity of coronary artery disease. J Geriatr Cardiol 2013;10:34-8.
24. Zhao Y, Ponnusamy M, Zhang L, et al. The role of miR-214 in cardiovascular diseases. Eur J Pharmacol 2017;816:138-45.
25. Xu JZ, Shao CC, Wang XJ, et al. circTADA2As suppress breast cancer progression and metastasis via targeting miR-203a-3p/SOCS3 axis. Cell Death Dis 2019;10:175.

26. Černá V, Ostašov P, Pitule P, et al. The Expression Profile of MicroRNAs in Small and Large Abdominal Aortic Aneurysms. Cardiol Res Pract 2019;2019:8645840.
27. Jin Y, Pang T, Nelin LD, et al. MKP-1 is a target of miR-210 and mediate the negative regulation of miR-210 inhibitor on hypoxic hPASMC proliferation. Cell Biol Int 2015;39:113-20.
28. Hansson GK. Inflammation, atherosclerosis, and coronary artery disease. N Engl J Med 2005;352:1685-95.
29. Wong ND, Zhao Y, Quek RGW, et al. Residual atherosclerotic cardiovascular disease risk in statin-treated adults: The Multi-Ethnic Study of Atherosclerosis. J Clin Lipidol 2017;11:1223-33.
30. Raposeiras-Roubin S, Rosselló X, Oliva B, et al. Triglycerides and Residual Atherosclerotic Risk. J Am Coll Cardiol 2021;77:3031-41.
31. Ridker PM. How Common Is Residual Inflammatory Risk? Circ Res 2017;120:617-9.
32. Wang W, Sheng L, Chen Y, et al. Total coumarin derivates from Hydrangea paniculata attenuate renal injuries in cationized-BSA induced membranous nephropathy by inhibiting complement activation and interleukin 10-mediated interstitial fibrosis. Phytomedicine 2022;96:153886.
33. Ross R. Atherosclerosis is an inflammatory disease. Am Heart J 1999;138:S419-20.
34. Barwari T, Rienks M, Mayr M. MicroRNA-21 and the Vulnerability of Atherosclerotic Plaques. Mol Ther 2018;26:938-40.
35. Yu DR, Wang T, Huang J, et al. MicroRNA-9 overexpression suppresses vulnerable atherosclerotic plaque and enhances vascular remodeling through negative regulation of the p38MAPK pathway via OLR1 in acute coronary syndrome. J Cell Biochem 2020;121:49-62.
36. Tang Y, Yu S, Liu Y, et al. MicroRNA-124 controls human vascular smooth muscle cell phenotypic switch via Sp1. Am J Physiol Heart Circ Physiol 2017;313:H641-9.
37. Chistiakov DA, Bobryshev YV, Nikiforov NG, et al. Macrophage phenotypic plasticity in atherosclerosis: The associated features and the peculiarities of the expression of inflammatory genes. Int J Cardiol 2015;184:436-45.
38. Roycik MD, Myers JS, Newcomer RG, et al. Matrix metalloproteinase inhibition in atherosclerosis and stroke. Curr Mol Med 2013;13:1299-313.

Cite this article as: Jin Y, Lu J, Liu F, Yang X, Chen F, Zhang J. MiR-4291 stabilized the vulnerable atherosclerotic plaques by degrading the MAPK1/ERK2 in ApoE$^{-/-}$ mice. Ann Transl Med 2022;10(22):1243. doi: 10.21037/atm-22-5241

